JOURNAL OF MATERIALS SCIENCE 18 (1983) 3749–3755

Effects of subgrain structures and stress orientation on fatigue of brass

T. F. LIU, C. M. WAN, M. T. JAHN, S. C. CHANG
Department of Materials Science and Engineering, National Tsing Hua University, Hsinchu, Taiwan

Subgrain structures of 70 wt% copper – 30 wt% zinc brass were obtained by cold rolling and annealing. Effects of subgrain structure and orientation on fatigue properties were studied. It is found that the fatigue properties of the specimens with subgrains are superior to those of fully annealed specimens. The fatigue properties of specimens tested in the transverse direction (FT) are superior to those of specimens tested in the longitudinal direction (FL) for short annealing time. This result can be rationalized by the textured structre of the specimens in which both the resolved shear and normal stresses on the shear bands formed in FT specimens are smaller than those in FL specimens.

1. Introduction

The dislocation characteristics of a subgrain boundary and the form of the dislocation pile-up affect the tensile properties of a material [1–4]. The development of slip line changes with crystal orientation and so does the stress–strain diagram [5–7]. However, not much work has been done on fatigue properties as a function of subgrain structure and grain orientation.

In this work, the fatigue properties of materials with and without a subgrain structure were compared. Effects of fatigue stress orientation on fatigue mechanisms were also studied.

2. Experimental procedures

The as-received material was 70% copper–30% zinc brass sheet with a thickness of 3.5 mm. It was reduced in thickness of 75% by cold rolling to 0.875 mm. After rolling, materials were annealed in a 350° C salt bath for 2, 5, 10, 25, 50, 100 and 1000 sec to get a distribution of subgrain size.

Tensile tests were performed with an Instron Tensile Machine Model 1115 at a crosshead speed of 0.05 cm min^{-1}. For each annealing time, specimens for both the longitudinal (SL) and transverse (ST) directions were prepared.

A Sonntage Model SF-2-U fatigue testing machine with a frequency of bending stress of 1800 cycle min^{-1} was used for fatigue tests. Longitudinal and transverse fatigue specimens, named as FL and FT specimens, were also prepared. The number following the name of a specimen indicates the annealing time of it in seconds. All fatigue test samples were electrolytically polished before tests to minimize the surface effect. A JSM-U3 scanning electron microscope was used to examine the specimen free surface after fatigue test. Internal microstructure was investigated by a Jeol-100B transmission electron microscope.

3. Results

3.1. Microstructures before fatigue test

Average subgrain or cell sizes of specimens are shown in Fig. 1. Fig. 2 shows the tangled dislocations in the as-rolled specimen. Subgrains start to form in the specimen after 5 sec annealing. These subgrains then gradually grow with annealing time as shown in Fig. 3. Fig. 4 shows the microstructure of a specimen annealed for 50 sec. Almost all dislocations were annealed out as the annealing prolonged over 50 sec.

3.2. Tensile and fatigue properties

The room temperature tensile properties and fatigue lives of specimens in longitudinal and transverse directions are shown in Figs. 5 and 6. All fatigue tests were carried out at a cyclic stress of $\sigma_{ap} = 42.5\,kg\,mm^{-2}$. Fig. 6 indicates that the

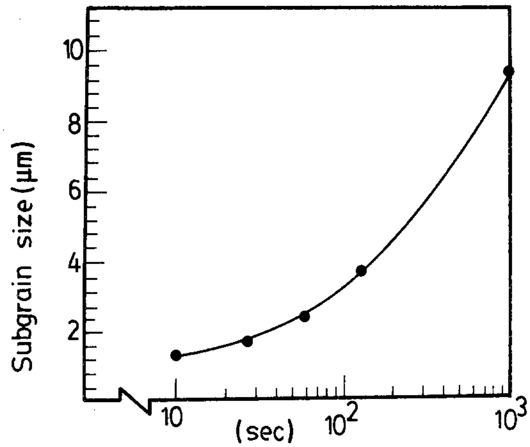

Figure 1 Variation of subgrain size with annealing time.

fatigue life of specimen FL 10 is much longer than that of specimen FL 1000. In general, fatigue lives of specimens decrease with increase of annealing time. The fatigue life of specimen FT is longer than that of specimen FL when the annealing time is shorter than 25 sec. For longer annealing time, the reverse is true.

3.3. Free surface morphology

3.3.1. Slip band cracks

Figs. 7 to 12 show the SEM morphology of free surfaces of fatigued specimens. As shown in Fig. 7, fatigue-induced slip bands in a grain were developed along the direction 55° to the applied fatigue stress on specimen FL 10 and accomodate boundaries were formed. Intrusions and extrusions were associated with slip bands. At the roots of intrusions some microcracks were initiated. There are dense slip bands in many different directions on the fully annealed specimen FL 1000 after fatigue. Fig. 8 shows that microcracks formed at the intersection of these dense slip bands. These microcracks propagated and linked with each other along different slip bands or grain boundaries.

The free surface of an as-rolled specimen FL after being fatigued in the longitudinal directions is shown in Fig. 9. In general, the slip bands are in the direction about 55° to the applied fatigue stress. In Fig. 9, the boundary separating two sets of slip bands which make an angle of 110° is a twin boundary. The cracks along different slip bands linked with each other. Fig. 10 indicates duplex slip bands of two directions about 20° and 35° to the applied fatigue stress on the free surface of the as-rolled specimen FT after being fatigued in the transverse direction. Microcracks were formed at the intersections of these slip bands.

Figs. 11 and 12 reveal slip bands on specimen FT 10. They are similar to the slip bands on the

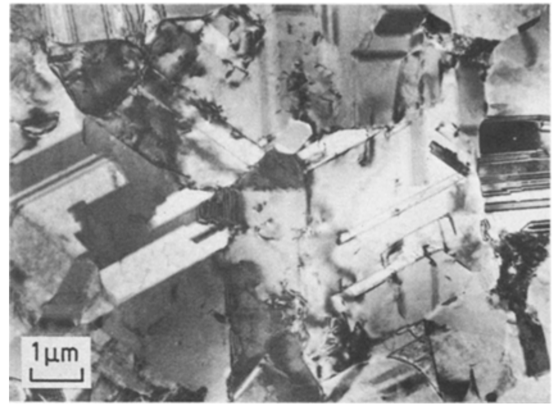

Figure 3 The microstructure of a specimen annealed at 350° C for 10 sec after cold rolling (TEM).

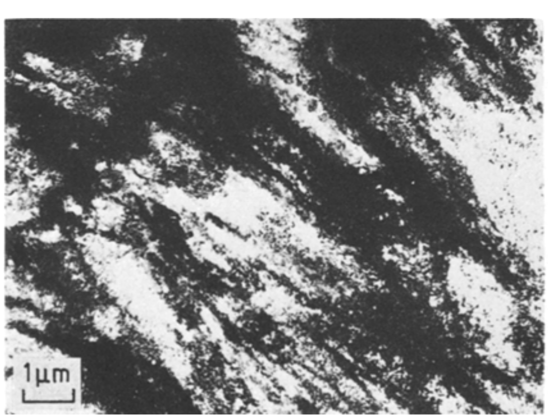

Figure 2 The microstructure of a specimen with 75 per cent reduction in thickness by cold rolling (TEM).

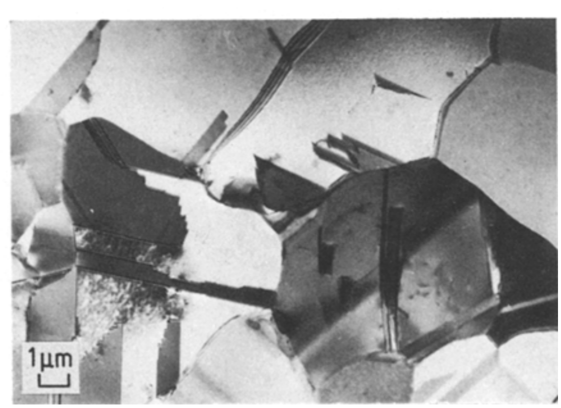

Figure 4 The microstructure of a specimen annealed at 350° C for 50 sec after cold rolling (TEM).

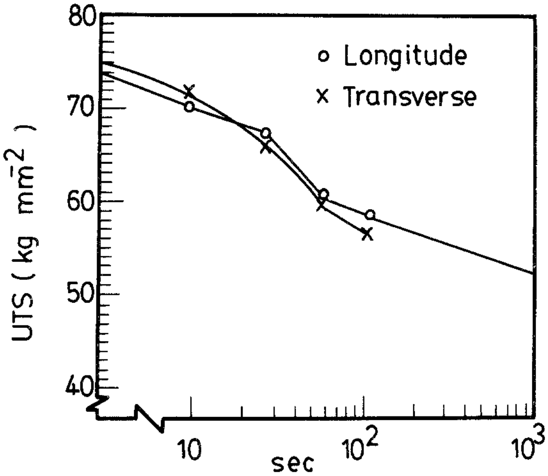

Figure 5 Decrease in UTS as a function of annealing time.

as-rolled specimen FT. Some microcracks also originated at the intersection of two slip bands, linked with one another, and propagated along one or another slip band. Slip bands were sheared by each other at their intersections as shown in Fig. 12.

3.3.2. Grain boundary cracks

Fig. 8 indicates that two densely distributed slip bands of grain A and grain B impinged compactly and no crack was found on the grain boundary. However, cracks formed on the grain boundary between grain C and grain D in which the densities of slip bands were quite different and the slip bands in grain C were almost paralleled to the crack grain boundary between grain C and grain D. Cracks also formed along the grain boundary

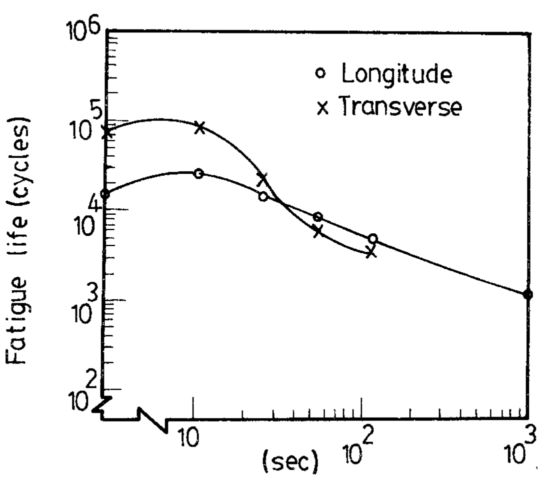

Figure 6 Fatigue lives of specimens as a function of different annealing time.

between grain E and grain F, even their slip-band orientation was quite different from the grain boundary between them.

4. Discussion

In general, fatigue fracture process takes place in the sequence of (a) fatigue crack initiation, (b) the first stage fatigue crack growth, and (c) the second stage fatigue crack growth [8, 9]. The first stage fatigue crack growth involves cyclic shearing along planes of high resolved shear stress and can be considered as an extension of the slip band intrusion (initiation) process. The second stage fatigue crack growth is mainly controlled by the normal stress at the crack tip.

It has been reported [5] that slip bands, grain boundaries and twin boundaries are major crack initiation sites. In this work, the former two types of sites were observed.

The rolling textures in fcc metals and alloys are known to vary with the composition and temperature of deformation. For Cu–30% Zn brass rolled at room temperature, there are five major stages in the texture development [10, 11]. However, it is found that after a heavy reduction as in this work, the rolling texture is the typical α-brass-type texture $\{110\}\langle 112\rangle$.

For a fully annealed specimen, the recrystallized texture is very diffuse [12], and there is a large spread in orientation of the grains. As shown in Fig. 8, the slip lines in different grains are along different directions. Therefore, there are large incompatible strains between grains caused by the pile-up of dislocations at a grain boundary where cracks would nucleate and propagate. On the other hand, for specimens with a subgrain structure (annealed for a short time), the tendency for the formation of grain boundary cracks are largely reduced. The reasons are: first, the dislocation pile-up is smaller for smaller subgrain sizes and second, for a specimen annealed for only a short time, the retained rolling texture implies a relatively small misorientation between subgrains which permits slip bands to propagate through the boundaries without much difficulty. This point of view can be verified by looking at Fig. 7 and Fig. 9, and it explains the observation that the fatigue lives of specimens decrease as the annealing time increases.

Samuels [13] and Samuels and Hatherly [14] observed the metallographic slip-line indications on deformed Cu–30% Zn brass specimens and

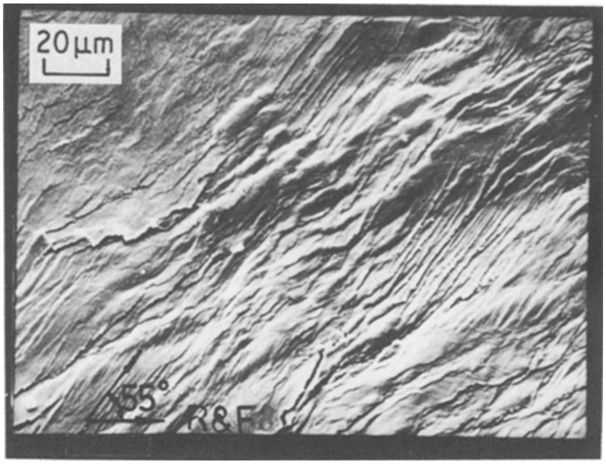

Figure 7 The free surface of the fatigued sample FL 10 (SEM).

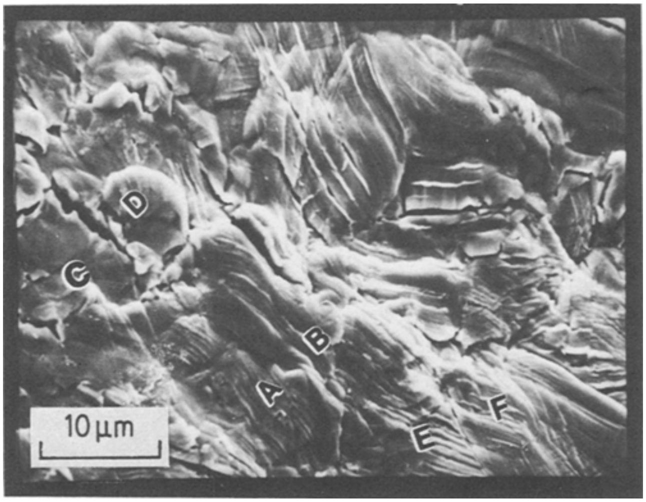

Figure 8 The free surface of the fatigued sample FL 1000 (SEM).

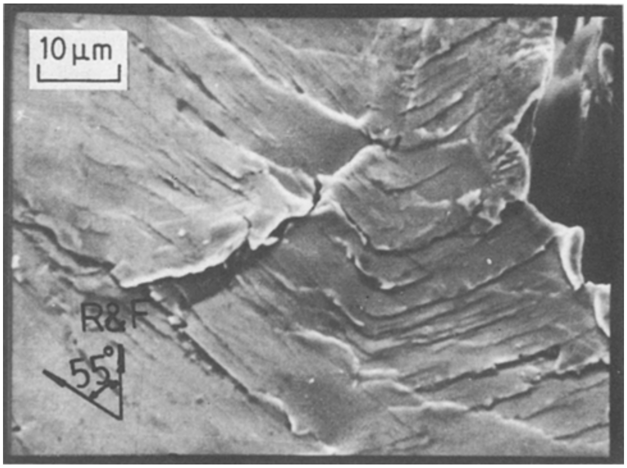

Figure 9 The free surface of the as-rolled (FL) specimen after fatigue test (SEM).

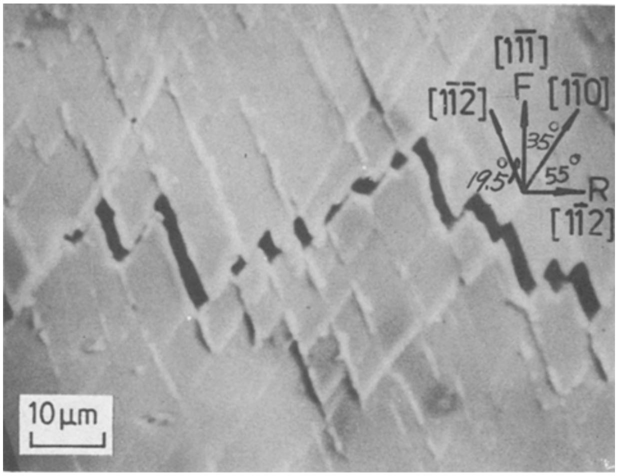

Figure 10 The free surface of the as-rolled (FT) specimen after fatigue test (SEM).

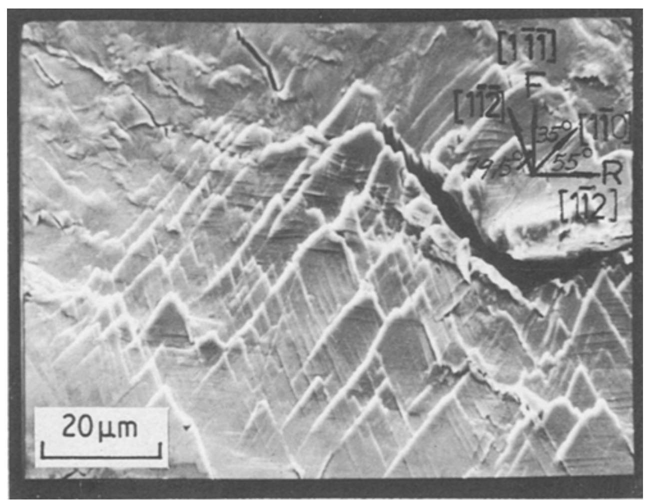

Figure 11 The free surface of the fatigued sample FT 10 (SEM).

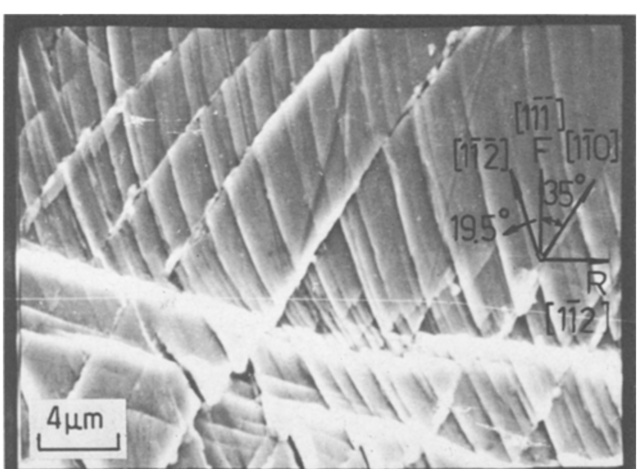

Figure 12 The free surface of the fatigued sample FT 10 (SEM).

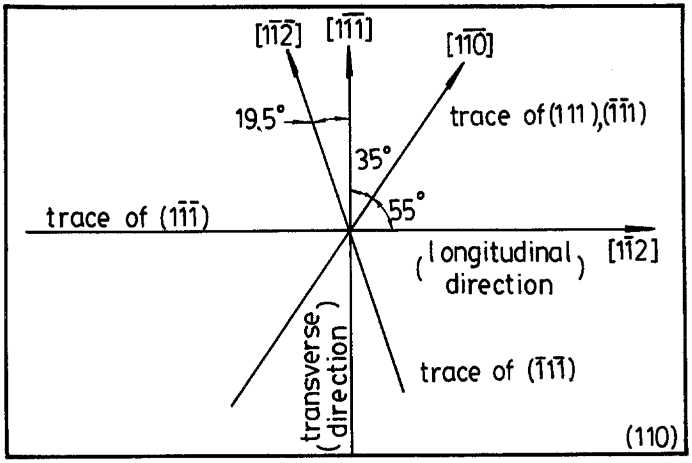

Figure 13 Traces of $\{1\,1\,1\}$ slip planes on $(1\,1\,0)$ plane.

found them as $\{1\,1\,1\}$ traces. Fig. 13 shows the $(1\,1\,0)$ plane in a cubic crystal. The traces of possible slip planes: $(\bar{1}\,1\,\bar{1})$, $(1\,\bar{1}\,\bar{1})$, $(\bar{1}\,\bar{1}\,1)$ and $(1\,1\,1)$ on $(1\,1\,0)$ are $[1\,\bar{1}\,\bar{2}]$, $[1\,\bar{1}\,2]$, $[1\,\bar{1}\,0]$ and $[1\,\bar{1}\,0]$, respectively. For specimen tested in the longitudinal directions, the maximum normal stress σ lies along $[1\,\bar{1}\,2]$. From the calculation of resolved normal stress and shear stress [15], it is found that for all possible slip systems $\{1\,1\,1\}\langle 1\,1\,0\rangle$ in a fcc structure, the largest resolved shear stress is along the slip systems $(1\,1\,1)$ $[\bar{1}\,0\,1]$ and $(\bar{1}\,\bar{1}\,1)$ $[1\,0\,1]$ in which the resolved shear stress $\tau_l = (1/6^{1/2})\sigma$, and the resolved normal stress, $\sigma_l = (2/9)\sigma$. From Fig. 13, one finds that the traces of both $(1\,1\,1)$ and $(\bar{1}\,\bar{1}\,1)$ on $(1\,1\,0)$ are $[1\,\bar{1}\,0]$ which makes an angle of 54.73° with the longitudinal direction $[1\,\bar{1}\,2]$. This is consistent with the observations on FL 10 and FL specimens (Figs. 7 and 9). The two sets of slip bands shown in Fig. 9 are formed by twinning. The twin plane is $(1\,\bar{1}\,\bar{1})$ whose trace on $(1\,1\,0)$ is the longitudinal direction $[1\,\bar{1}\,2]$.

For specimens tested in the transverse direction, the maximum normal stress lies along $[\bar{1}\,1\,1]$. From the calculation of resolved normal stress and shear stress, it is found that the largest resolved shear stress is along slip systems $(1\,1\,1)[1\,\bar{1}\,0]$, $(1\,1\,1)[\bar{1}\,0\,1]$, $(\bar{1}\,\bar{1}\,1)[1\,\bar{1}\,0]$, $(\bar{1}\,\bar{1}\,1)[0\,1\,1]$, $(\bar{1}\,1\,\bar{1})$ $[0\,1\,1]$ and $(\bar{1}\,1\,\bar{1})[\bar{1}\,0\,1]$ in which the resolved shear stress $\tau_t = [2/3(6)^{1/2}]\sigma$ and the resolved normal stress $\sigma_t = (1/9)\sigma$. As shown in Fig. 13, the traces of both $(1\,1\,1)$ and $(\bar{1}\,\bar{1}\,1)$ on $(1\,1\,0)$ are $[1\,\bar{1}\,0]$ while the trace of $(\bar{1}\,1\,\bar{1})$ on $(1\,1\,0)$ is $[1\,\bar{1}\,\bar{2}]$. The angles between $[1\,\bar{1}\,0]$, $[1\,\bar{1}\,\bar{2}]$ and $[\bar{1}\,1\,1]$ are shown in Fig. 13, which are exactly the angles between shear bands and fatigue directions in specimens tested along the transverse direction (Figs. 10 to 12). Both the largest resolved shear and normal stresses in a specimen tested along transverse direction are smaller than those in a specimen tested along the longitudinal direction. This result explains the fact that for a short annealing time the fatigue properties of specimens tested in the transverse direction are superior to those of specimens tested in the longitudinal direction.

5. Conclusions

1. The fatigue properties of Cu–30% Zn specimens with pre-existing subgrains are superior to those of fully annealed specimens. This could be explained by the smaller tendency of formation of grain boundary cracks in a specimen with a subgrain structure.

2. After 75% reduction by cold rolling at room temperature, the microstructure is highly textured. The typical $\{1\,1\,0\}\langle 1\,1\,2\rangle$ rolling texture will be retained after annealing at 350° C for short time ($\leqslant$25 sec).

3. For specimens annealed at 350° C for less than 25 sec, the fatigue cracks take place mainly along slip bands. The slip bands are along traces of $\{1\,1\,1\}$ slip planes on $\{1\,1\,0\}$ sheet plane. For specimens tested in longitudinal directions, the slip bands are mainly 54.73° to the stress direction. For specimens tested in transverse directions, two family of slip bands were observed. They make angles 19.47° and 35.26° to the stress direction and form an angle of 54.73° with each other.

4. The fatigue properties of specimens tested in the transverse direction are superior to those tested in the longitudinal direction, which can be explained by the smaller resolved shear and normal stresses on possible slip systems in a highly textured $\{1\,1\,0\}\langle 1\,1\,2\rangle$ structure.

References

1. A. W. THOMPSON and W. A. BACKOFEN, *Acta Metall.* **19** (1971) 597.
2. *Idem, Met. Trans.* **2** (1971) 2004.
3. D. KALISH and B. G. LEFEVRE, *ibid.* **6A** (1975) 1319.
4. H. J. McQUEEN, *ibid.* **8A** (1977) 807.
5. F. D. ROSI, *J. Mater. Sci.* **8** (1973) 807.
6. M. MASIMA and G. SACHS, *Z. Phys.* **50** (1928) 161.
7. V. GOLER and G. SACHS, *ibid.* **55** (1929) 581.
8. A. N. MAY, *Nature* **185** (1960) 303.
9. E. SCHMID and W. BOAS, "Kristall Plastizitat" (Julius Springeri, Berlin, 1935) p. 148.
10. B. J. DUGGAN, M. HATHERLY, W. B. HUTCHINSON and P. T. WAKEFIELD, *Met. Sci.* **12** (1978) 343.
11. W. B. HUTCHINSON, B. J. DUGGAN and M. HATHERLY, *Met. Technol.* **6** (1979) 398.
12. B. J. DUGGAN, W. B. HUTCHINSON and M. HATHERLY, *Scripta Metall.* **12** (1978) 293.
13. L. E. SAMUELS, *J. Inst. Met.* **83** (1955) 359.
14. L. E. SAMUELS and M. HATHERLY, *J. Inst. Met.* **84** (1955) 84.
15. C. S. HARTLEY and J. P. HIRTH, *TMS-AIME* **233** (1965) 1415.

Received 8 February and accepted 22 April 1983